Dopamine release in nucleus accumbens during rewarded task switching measured by [11C]raclopride

Lars S. Jonasson [a,b,c,*], Jan Axelsson [a], Katrine Riklund [a,b], Todd S. Braver [d], Mattias Ögren [a], Lars Bäckman [e], Lars Nyberg [a,b,f]

[a] Department of Radiation Sciences, Umeå University, SE-901 87 Umeå, Sweden
[b] Umeå Center for Functional Brain Imaging (UFBI), Umeå University, SE-901 87 Umeå, Sweden
[c] Centre for Population Studies, Ageing and Living Conditions, Umeå University, SE-901 87 Umeå, Sweden
[d] Department of Psychology, Washington University, St Louis, MO 63130, USA
[e] Aging Research Center, Karolinska Institute, SE-113 30 Stockholm, Sweden
[f] Department of Integrative Medical Biology, Physiology, Umeå University, SE-901 87 Umeå, Sweden

ARTICLE INFO

ABSTRACT

Reward and motivation have positive influences on cognitive-control processes in numerous settings. Models of reward implicate corticostriatal loops and the dopamine (DA) system, with special emphasis on D_2 receptors in nucleus accumbens (NAcc). In this study, 11 right-handed males (35–40 years) were scanned with positron emission tomography (PET) in a single [11C]raclopride dynamic scan during rewarded and non-rewarded task switching. Rewarded task switching (relative to baseline task switching) decreased [11C]raclopride binding in NAcc. Decreasing NAcc [11C]raclopride binding was strongly associated with task reaction time measures that reflect individual differences in effort and control strategies. Voxelwise analyses additionally revealed reward-related DA release in anterodorsal caudate, a region previously associated with task-switching. These PET findings provide evidence for striatal DA release during motivated cognitive control, and further suggest that NAcc DA release predicts the task reaction time benefits of reward incentives.

Introduction

Reward, intrinsic or extrinsic, can influence motivation (Pessoa, 2009), reinforce behavior (Niv et al., 2007), and improve cognitive processing (Beierholm et al., 2013; Krebs et al., 2012; Shen and Chun, 2011). Recent functional magnetic resonance imaging (MRI) studies have also demonstrated that reward increase blood-oxygenation-level-dependent (BOLD) responses in limbic regions throughout the brain (Knutson et al., 2005; Small et al., 2005). Subcortically, the mesolimbic dopamine (DA) system and the nucleus accumbens (NAcc) in particular are at the core of several reward frameworks (Haber and Knutson, 2010; Niv et al., 2007; Sarter et al., 2006), involved in coding prediction errors (Schultz, 1998), influencing action (Niv et al., 2007; Salimpoor et al., 2013), and allocating attentional resources (Pessoa, 2009; Sarter et al., 2006).

Positron emission tomography (PET) investigations on D_2-receptor binding, with [11C]raclopride as an index of DA release (Laruelle, 2000) in striatum, have implicated the ventral striatum (VS; for a review see Egerton et al., 2009). The relatively few published studies focusing on monetary reward effects vary considerably in their design, choice of tasks, control conditions, and results (Egerton et al., 2009; Martin-Soelch et al., 2011; Urban et al., 2012). Several used choice reaction-time (RT) tasks (Pappata et al., 2002; Schott et al., 2008; Urban et al., 2012), or tasks for which reward acquisition was independent of performance (Hakyemez et al., 2008; Martin-Soelch et al., 2011; Zald et al., 2004), and one study used a video game task (Koepp et al., 1998). Only two investigations reported associations between a change in DA release and performance, such that one observed a significant relationship (Koepp et al., 1998) whereas the other did not (Urban et al., 2012). A reason for the positive finding may be that Koepp et al. (1998) associated performance with a continuously rewarding task contrasted against a passive baseline. However, reanalysis by Egerton et al. (2009) revealed that applying motion correction to that data removed the association. An explanation for the prior null finding may be that earning reward did not require sufficient effort and/or cognitive control to be translated into a change in the non-displaceable binding potential (BP_{ND}) of [11C]raclopride. Another reason may be that the task measure related to BP_{ND} was not sensitive enough, which would suggest a need for further investigations of DA release in rewarding contexts. The aim of the present study was to investigate the effects of

* Corresponding author at: Department of Radiation Sciences, Diagnostic Radiology, Umeå University, SE-901 87 Umeå, Sweden.
E-mail address: lars.jonasson@diagrad.umu.se (L.S. Jonasson).

reward in striatum using a task with high cognitive control demands. The choice of a more demanding cognitive control task may be more suitable for investigating the influence of NAcc DA release on attentional effort and task performance.

Several reports have shown that reward related improvements on task RT may be transferred to non-rewarded trials (R$^-$) intermingled with rewarded trials (R$^+$) (Beierholm et al., 2013; Jimura et al., 2010). These effects have also been associated with increased DA levels (Beierholm et al., 2013). The Dual Mechanisms of Control (DMC) framework (Braver et al., 2007) provides an account of such effects in terms of a shift in cognitive control mode: In task conditions with high-reward value, reward maximization can be achieved by shifting toward sustained but more resource-demanding proactive control processing in the prefrontal cortex (PFC; Jimura et al., 2010). Relatedly, these findings can be interpreted as depending on increased attentional effort mediated by NAcc DA (Sarter et al., 2006), allocating resources in frontal control networks and early sensory areas (Pessoa, 2009; Sarter et al., 2006). Integrating these two frameworks, NAcc could provide a striatal substrate for DMC (Braver et al., 2007), as a "motivational engine" (Knutson et al., 2003). Recent findings suggest that DA in NAcc could be linked to speeding of responses for a variety of reasons: increasing generalized drive and vigor (Niv et al., 2006), enhancing attentional effort (Sarter et al., 2006), or as a proxy indicator of higher tonic DA tone associated with a sustained (proactive) control mode (Braver, 2012).

In the present study, a rewarded cued task-switching paradigm with an active baseline was adopted. The task was selected to impose high cognitive control demands compared to previous investigations and an active rather than passive baseline condition was chosen to control for sensorimotor (Lappin et al., 2009) and task-switching (Monchi et al., 2006) influences on BP$_{ND}$ in the striatum. We assessed DA release with PET, and the reversible D$_2$ ligand [^{11}C]raclopride with a bolus plus constant infusion (B/I) protocol to compare conditions within a single dynamic PET scan (Watabe et al., 2000). Consequently, we probed the ability to detect subtle reward-induced changes in BP$_{ND}$ in a D$_2$ system already burdened by the cognitively demanding task itself (Monchi et al., 2006). Previous studies, with the exception of Schott et al. (2008), looked at the ventral striatum rather than the NAcc specifically. In order to target a small structure like NAcc, we used a spatial high-resolution iterative reconstruction method based on an Ordered Subsets Expectation Maximization (OSEM) algorithm (Ross and Stearns, 2010).

Based on the extant literature reviewed above, a number of hypotheses were formulated. First, compared to a no-reward baseline, task-switching with reward incentives was predicted to lead to a reduction in NAcc BP$_{ND}$ (Schott et al., 2008). Secondly, providing reward incentives during task switching was expected to reduce RT without a cost in accuracy (i.e. enhanced performance rather than a speed-accuracy shift; Jimura et al., 2010). Third, a key question of interest was whether ΔBP$_{ND}$ relates primarily to transient modulations of effort on R$^+$ trials, or to sustained effort throughout the rewarded (R) condition (Beierholm et al., 2013; Niv et al., 2006; Sarter et al., 2006). The change in NAcc BP$_{ND}$ was predicted to be associated with the degree of reward-related improvement in task performance, specifically for indices that reflected global sustained effort throughout the reward blocks (i.e., on R$^-$ as well as R$^+$ trials; Sarter et al., 2006). To test this hypothesis, two separate analyses were made. First, assuming that RT on R$^+$ trials reflects an individual's maximum effort to perform fast enough to acquire a reward, RT on R$^-$ trials can be viewed as representing the deviation from the maximum effort possible. Accordingly, a smaller RT difference between R$^+$ and R$^-$ trials within the rewarded condition is assumed to reflect increased attentional effort, and higher effort should result in a larger reduction of NAcc BP$_{ND}$ (Sarter et al., 2006). Second, as predicted by the DMC model (Braver et al., 2007) ΔBP$_{ND}$ should be positively correlated with the degree of improvement on R$^-$ trials relative to baseline (B $-$ R$^-$), but modulated by a scaling factor that reflects how much of the R$^-$ improvement reflects the total R$^+$ related improvement (i.e., [B $-$ R$^-$]/[B $-$ R$^+$]).

Methods

Participants

Thirteen males, between 35 and 40 years (M $= 38.0 \pm 1.7$) were recruited by means of a local newspaper advertisement in Umeå, Sweden. Inclusion criteria were: right handedness, normal color vision, and not taking prescription drugs affecting the brain. Participants were asked not to do heavy physical exercise the day before scanning. Two participants were excluded from analyses, one because of falling asleep repeatedly during scanning, and one for being unable to obtain even a single reward and showing signs of fatigue. Participants were paid 1250 SEK and could earn an additional 500 SEK depending on the number of collected rewards (equivalent to $200 and $80 respectively). This study was approved by the Regional Ethical Review Board in Umeå.

Procedure

Upon arrival, participants signed informed consent, followed by the creation and fitting of a thermoplastic mask used for minimizing head movements during scanning. After insertion of an injection needle, [^{11}C]raclopride was prepared, leaving 20 to 30 min for resting and task practice. Participants were instructed on the task and practiced for roughly 14 min. They were then positioned in the scanner, and five minutes after computerized tomography (CT) acquisition, the task was initiated. Time from arrival until the scan started was approximately 80 min. PET acquisition commenced five minutes after task onset.

PET

PET images were acquired in 3D mode using a Discovery 690 PET/CT (General Electric, WI, US), at the Department of Nuclear Medicine, Norrland's University Hospital. A low-dose helical CT scan (20 mA, 120 kV, 0.8 s/revolution), provided data for PET attenuation correction. Participants were injected with a bolus plus constant infusion (Kbol = 105 min, Watabe et al., 2000). The total [^{11}C]raclopride delivered was 250 MBq over 81 min of dynamic PET scanning. Thirty frames of varying duration were collected (8×2, 4×3, 2×4.33, 1×5.33, 2×3, 3×2.66, and 10×2.5 min). Attenuation- and decay-corrected 256×256-pixel transaxial PET images were reconstructed to a 25 cm field-of-view employing the Sharp IR algorithm (6 iterations, 24 subsets, 3.0 mm Gaussian post filter). Sharp IR is an advanced version of the OSEM method for improving spatial resolution, in which detector system responses are included (Ross and Stearns, 2010). The Full-Width Half-Maximum (FWHM) resolution is below 3 mm. The protocol resulted in 47 tomographic slices per time frame, yielding $0.977 \times 0.977 \times 3.27$ mm^3 voxels. Images were decay-corrected to the start of the scan. After scanning, images were exported and de-identified using the Dicom2Usb "one-click anonymization" hardware (http://dicom-port.com/).

Image processing and data analysis

SPM8 (http://www.fil.ion.ucl.ac.uk/spm/) was used for preprocessing. For each participant, all frames were realigned to the individual mean image. One subject's structural T1 image was available for MRI based alignment, as this individual had participated in an unrelated MRI project, acquired with a 3 T Phillips MRI scanner. This participant's mean PET image, averaged across all time-frames, was co-registered to the structural image which was normalized to the Montreal Neurological Institute (MNI) coordinate system (http://www.bic.mni.mcgill.ca/), using the ICBM 2009c nonlinear symmetric template (Fonov et al., 2009, 2011). The normalization parameters were then applied to the co-registered PET image. That PET image served as a template onto which all participants' PET images were normalized to $1 \times 1 \times 1$ mm^3 voxels. Using the Freesurfer segmentation software (http://surfer.nmr.

mgh.harvard.edu/), the normalized T1 image was segmented to create a brain atlas from which our three ROIs were extracted (NAcc, caudate, and putamen), as well as the cerebellar gray matter, which served as reference region. The method uses anatomical information from a T1 structural image for automatic segmentation and assigns an anatomical label to each voxel in a volume (Fischl et al., 2002). The original ROIs were thresholded at 30% of maximum intensity for each individual separately, producing subject-specific ROIs used for subsequent analyses. This was done in order to avoid inclusion of matter outside the striatum. Finally, ROIs were collapsed across the left and right hemispheres as we had no predictions regarding lateralization effects and because inter-hemispheric BP_{ND} correlations were high at baseline ($ps < .01$).

An in-house developed software, *Imlook4d* (http://dicom-port.com/), was used for obtaining tissue time–activity curves (TACs) for ROIs, and for creating BP_{ND} images for voxelwise analyses. BP_{ND} at equilibrium was calculated as; ($BP_{ND} = (C_{roi} - C_{ref})/C_{ref}$, Watabe et al., 2000). The decay-corrected radioactive concentration [Bq/ml] is annotated C_{roi} in the target region, and C_{ref} in the cerebellum serving as the reference region (Carson et al., 1997; Ito et al., 1998).

To determine when equilibrium had been reached, paired sample t-tests were performed on adjacent frames in the reference region (i.e. frame 1 relative to frame 2, frame 2 relative to frame 3, and so on). Each pair differed up to frame 16 ($p < .05$) whereas from frame 16 and onwards BP_{ND} did not differ significantly ($p > .05$). As we were particularly concerned with the relation between BP_{ND} and the task measures we wanted a comparison to be made with frames being as close together in time as possible, while giving time for the manipulation to influence binding (Watabe et al., 2000). Baseline data (BP_B) was obtained from 42 to 53.3 min (frames 16 to 19) and reward data (BP_R) between 58.5 and 71 min (frames 22 to 26). As frames 16 to 19 were decided by the demand to reach equilibrium, limiting the analyses in the R condition to frames 22 to 26 removed frames with higher noise, and kept the comparison conditions as close together in time as possible, while minimizing time-on-task asymmetries. In addition, frames 22–29 were compared to BP_B as a complementary analysis.

Task-switching

A cued task-switching paradigm was used (Fig. 1; Rogers and Monsell, 1995), developed in E-Prime Version 2.0 (Psychology Software Tools, Inc., Pittsburgh, PA). Before being positioned in the scanner, participants made a practice run of 118 trials, and their median RT on accurate trials was used as the criterion time for rewarded trials (R^+)

in the following PET scan. On each trial, the sequence of events was as follows: fixation cross (1000 ms), task cue (250 ms), cue-target interval (1500 ms), and target (2000 ms). Task cues indicated the upcoming task, "Attend Letter" or "Attend Digit", the former indicating a consonant-vowel judgment, and the latter an odd-even judgment. Responses were indicated using one of two buttons with the thumb or right index finger on a custom-made two-button response box. The task cues were randomly alternated, such that there were a task switch on 50% of the trials, and a task-repeat on the other 50%. The target consisted of a letter-digit pair, with visual feedback given after the response, indicating whether it was correct (green square), an error (red triangle), or too slow ("Attend to the next trial" for responses not made within the 2000 ms response window).

The first six blocks were non-reward blocks (1×118, 5×75 trials), each separated by 30 s of rest. Fifty-four minutes into the scan, at the end of block 6, following 30 s of rest, instructions were presented for 25 s, notifying participants about the possibility of earning monetary reward on a subset of the upcoming trials. Reward incentive (R^+) trials were indicated when the task-cue appeared on a magenta-colored background, and no-reward (R^-) trials were indicated by the task cue appearing on a gray background. On R^+ trials, a bonus of 5 SEK (approx. 1 USD) was given for accurate responses faster than the RT cutoff (median correct RT from pre-scan practice), and was indicated via a distinct feedback screen presenting a picture of a 5 SEK coin. Participants then performed two additional rewarded task-switching R blocks to end the session (2×111 trials). The dependent measures were accuracy and RT. For RT, only accurate trials were included in analyses.

Statistical Analyses

ROI based analyses

The changes in BP_{ND} in NAcc, caudate, and putamen ROIs were analyzed with paired t-tests comparing BP_B to BP_R. The threshold for significance was adjusted for three ROIs ($p < .017$).

PET voxelwise analyses

In addition to the analysis of ROIs, voxelwise analyses were performed in SPM8 using paired t-tests on the striatal volumes. It is well established that the striatum can be divided functionally into the limbic (LST), associative (AST), and sensorimotor (SMST) striatum (Martinez et al., 2003). These functional subdivisions are not readily captured in the analysis of ROIs which are delineated based on anatomy. However, from voxelwise analyses it is possible to examine changes in specific
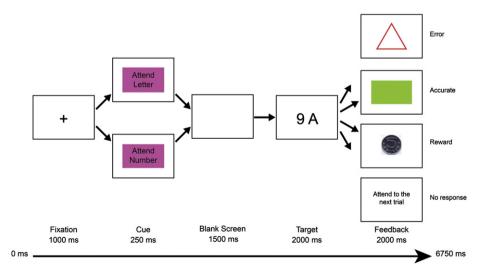

Fig. 1. Illustration of the task-switching paradigm. A fixation cross was presented for 1000 ms before a cue was presented for 250 ms stating the rule for that particular trial. Following a 1500 ms blank screen, the target stimulus was presented together with a trial-irrelevant stimulus for 2000 ms. Regardless of the response, a feedback screen was presented for 2000 ms indicating performance on each trial.

Table 1
Task performance and binding potential in baseline and reward conditions (Mean ± SD).

Condition	Task[a]		ROI[b]		
	RT	Accuracy	NAcc	Caudate	Putamen
Baseline	991 ± 199	92 ± 8	2.43 ± .30	2.76 ± .29	3.25 ± .28
Reward	832 ± 186	88 ± 11	2.30 ± .27	2.72 ± .31	3.23 ± .29

[a] Reaction time (RT) is reported in ms, accuracy in %.
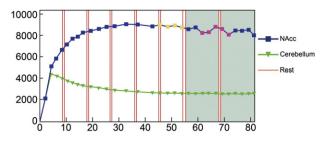[b] Regions of interest in BP_{ND}.

Fig. 3. Tissue time–activity curves for NAcc and cerebellum in blocks and frames. The decay-corrected radioactivity concentration is plotted along the time axis, NAcc in blue, and cerebellum in green. The vertical red lines delineate the blocks, separated by rest, and the shaded area delineates reward blocks. End points of baseline frames (16–19) are colored in yellow, and reward frames (22–26) in magenta.

functional regions (Lappin et al., 2009). Because of a strong a priori hypothesis regarding NAcc, which is a small region, we used relatively small voxels and low smoothing compared to previous investigations. BPND images were smoothed with a 4 mm FWHM kernel, yielding an effective smoothing kernel of 5.6 × 5.6 × 7.1 mm. A larger kernel would have introduced substantial partial volume effects in NAcc from putamen and caudate. An uncorrected statistical threshold of p < .005 was set, and a striatal small-volume correction was done by centering 8 mm diameter spheres on the peak activation foci (Knutson et al., 2005). These foci were considered significant if falling below the p < .05 level after correcting for multiple comparisons applying Gaussian Family-Wise Error (FWE) correction.

Correlations between reaction time and [11C]raclopride ΔBP_{ND}

Two-tailed Pearson correlations were used to test for the association between individual differences in NAcc ΔBP_{ND} and task RT measures. To control for variance not associated with the reward manipulation, changes were transformed into percentage change relative to baseline: $\Delta BP_{ND} = (1 - BPR/BPB) \times 100\%$ (Innis et al., 2007); RT improvements from baseline $= (1 - R/B) \times 100\%$; R RT difference score $= (1 - R^+/R^-) \times 100\%$; Scaled R^- improvement $(1 - R-/B) \times [(B-R)/(B-R^+)] \times 100$. Note that, apart from being relative, an increase in ΔBP_{ND} is analogous to a decrease in BP_{ND}. Additionally, although no such relation was expected, correlations between task RT and caudate and putamen ΔBP_{ND} were made to understand the specific relation between task RT and NAcc ΔBP_{ND}. The threshold for significance was adjusted for three comparisons to NAcc (p < .017).

Results

Task-switching

Means and SDs for task performance and BP_{ND} from frames 16–19 and 22–26 are reported in Table 1 (see Figs. 2 and 3 for visualization of the whole experiment). As expected, there was a marked reduction in average RT from the B to R block, t (10) = 5.94, p < .01. Accuracy remained fairly stable across conditions, t (10) = 1.23, p = .25.

Acquisition of reward was generally high, with participants obtaining 77% of available rewards on average.

ROI-based analyses

Confirming the main hypothesis, a significant reduction in NAcc BP_{ND} was seen during the reward condition, [t (10) = 3.33, p < .01], and the average ΔBP_{ND} per participant was 5.19% ± 5.07%. The other striatal ROIs yielded non-significant results: caudate [t (10) = 1.83, p = .10] and putamen [t (10) = .76, p = .47]. Fig. 3 displays NAcc and cerebellum TACs (see Inline Supplementary Figure S1 for participant-specific BP_{ND} values under both conditions). Using the longer interval (frames 22–29) yielded a significant reduction of BP_{ND} in NAcc [t (10) = 3.513, p = .01] and a trend in caudate [t (10) = 2.492, p = .03], but not putamen [t (10) = 1.946, p = .21].

Inline Supplementary Fig. S1 can be found online at http://dx.doi.org/10.1016/j.neuroimage.2014.05.047.

Voxelwise analyses

Voxelwise analyses yielded five significant clusters with decreased BP_{ND} for the baseline vs. reward contrast. Peak activation foci are reported in Table 2, and imposed on the ICBM2009c T1 template in Fig. 4. One cluster was located in left NAcc (Fig. 4A), one in left rostrodorsal caudate (Fig. 4B) and one in right rostrodorsal caudate, the former belonging to limbic striatum (LST), and the latter two being part of associative striatum (AST; Martinez et al., 2003). Finally, there were smaller, albeit significant, clusters in right ventrocaudal putamen, corresponding to sensorimotor striatum (SMST), and in right anteroventral putamen in LST (Martinez et al., 2003). Only one cluster had higher BP_{ND} during the rewarded condition — this cluster was located in right putamen along the anterior commissure plane.
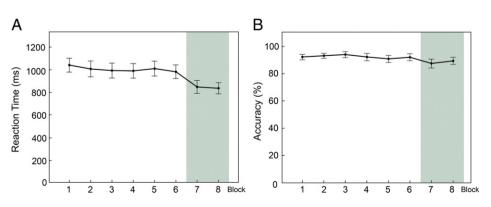

Fig. 2. Average reaction times and accuracy across blocks. In A–B, block numbers are shown on the x-axes, with the shaded area showing when reward trials were introduced. The y-axis in (A) depicts reaction time in ms, for correct responses, and (B) depicts accuracy (%). Error bars represent 1 SE.

Table 2

Peak activation foci in regions with altered BP$_{ND}$ in response to reward in MNI space with small-volume family-wise error correction.

	Region[a]	MNI coordinates[b]			t	p[c]	Voxels[d]
		X	Y	z			
B > R	L NAcc (LST)	−7	16	−5	4.64	.031	97*
	L Caudate (AST)	−13	10	12	8.67	.012	81*
	R Caudate (AST)	15	5	18	4.63	.032	60*
	R Putamen (SMST)	29	−14	−7	4.59	.033	28*
	R Putamen (LST)	20	13	−4	4.47	.037	10*
R > B	R Putamen	36	1	0	4.39	.040	24*

[a] Within parentheses following the region, an approximate functional localization according to Martinez et al. (2003) is given; associative striatum (AST), limbic striatum (LST), sensorimotor striatum (SMST).
[b] Coordinates are according to the MNI system.
[c] p-values are small-volume family-wise error corrected.
[d] Voxel size is 1 × 1 × 1 mm³.
* Peak activation foci significant at p < .001 uncorrected.

Correlations between reaction time and [11C]raclopride ΔBP$_{ND}$

Table 3 presents RT differences between conditions and trial types, and Fig. 5 shows scatter plots relating differences in RT to changes in ΔBP$_{ND}$ from baseline to reward. The decrease in RT from the B to R block was not related to NAcc ΔBP$_{ND}$ [r (9) = .18, p = .61] (Fig. 5A). However, counter to a transient effort account, ΔBP$_{ND}$ was strongly negatively rather than positively correlated with the R$^+$/R$^-$ RT difference in performance [r (9) = -.78, p < .01] (Fig. 5B). Additionally, consistent with a sustained effort account, ΔBP$_{ND}$ was positively correlated with the B/R$^-$ RT difference when this accounted for a large proportion of the total reward related benefit in RT [r (9) = .66, p = .03], although this analysis did not survive correction for multiple comparisons. The effects were specific to the NAcc. ΔBP$_{ND}$ in neither caudate nor putamen was related to either measure (p > .05).

Discussion

Using a task with high cognitive control demands and an active baseline we investigated reward related DA release in vivo with the D$_2$ tracer [11C]raclopride. The primary prediction was confirmed, namely that NAcc BP$_{ND}$ decreased when reward was offered for successful (i.e., fast and accurate) behavioral performance. This observation is likely due to DA release in NAcc, reducing D$_2$ receptor sites available to [11C]raclopride binding (Koepp et al., 1998; Laruelle, 2000). Previous studies

Table 3

Differences in reaction time between baseline and reward-context trials (Mean ± SD).

	B[c]			R[d]
	R	R$^+$	R$^-$	R$^+$/R$^-$
RT[a]	832 ± 186	765 ± 148	901 ± 241	
RT[b]	16.08 ± 8.57	22.16 ± 9.95	9.82 ± 10.18	13.09 ± 11.02

[a] Reaction time (RT) for different trial types in ms.
[b] RT differences between trial types are reported in %.
[c] In the middle, baseline (B) RT is compared to RTs on rewarded (R$^+$) and non-rewarded (R$^-$) trials within the reward condition (R).
[d] On the right, the RT difference-score is shown.

have used less demanding (Pappata et al., 2002; Schott et al., 2008; Urban et al., 2012) or non-cognitively demanding tasks (Hakyemez et al., 2008; Martin-Soelch et al., 2011; Zald et al., 2004). We observed an effect of reward in NAcc despite utilizing a task known to tax the striatal dopamine system even under non-rewarded task conditions (Monchi et al., 2006). In a pioneering study, Schott et al. (2008) found a convergence between NAcc [11C]raclopride ΔBP$_{ND}$ and BOLD signal in VS and ventral midbrain. Thus, a natural assumption is that our finding of NAcc DA release is similarly driven primarily by dopaminergic projections from the ventral tegmental area (Haber et al., 2000). Information transfer is complex however, and dynamic causal modeling has shown that reward information enters striatum from PFC before projecting back (Ballard et al., 2011), and NAcc both receives and sends projections to the ventral midbrain and other striatal regions (Haber et al., 2000). Thus, it is possible that reward effects in NAcc reflect a top-down influence from PFC regions.

In BOLD functional MRI studies, preparatory NAcc activation has been observed during the anticipatory gap between presentation of a reward cue and presentation of the target (Knutson et al., 2005). Previous [11C]raclopride investigations have used longer anticipatory gaps, above 5000 ms (Schott et al., 2008; Urban et al., 2012), supposedly increasing DA release, similar to increasing the BOLD response (Knutson et al., 2005). Despite a shorter 1750 ms anticipatory gap, we were able to detect a reduction in NAcc BP$_{ND}$ (see also Pappata et al., 2002). The observed ΔBP$_{ND}$ (M = 5.19%) falls within the range expected from previous reports (1% to 13.9%, Egerton et al., 2009; Martin-Soelch et al., 2011; Urban et al., 2012).

Although we were primarily focused on NAcc, other striatal regions were also sensitive to reward. The striatum influences cognitive control by DA, serving to update representations in PFC (Dahlin et al., 2008; O'Reilly and Frank, 2006). Updating of task stimuli, current rules, and
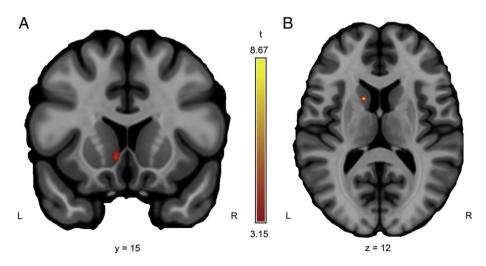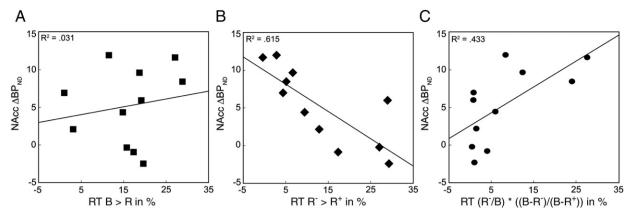

Fig. 4. Significant clusters of activation in left NAcc and caudate from SPM voxelwise analyses for baseline > reward. T-statistic maps generated in SPM were overlaid on the ICBM2009c non-linear symmetric T1 template in mriCron (http://www.nitrc.org/projects/mricron/). The colorbar reflects *t*-values. (A) Shows the cluster in left NAcc, and (B) the cluster in left dorsal caudate.

Fig. 5. Scatter plots depicting the relation between ΔBP_{ND} in NAcc and RT differences (in %). In A–C, linear fit lines have been inserted, and the corresponding R^2 is presented in the upper-left corner of each figure. ΔBP_{ND} in NAcc is plotted against: (A) the difference in RT between baseline and reward conditions, (B) the difference in RT between rewarded and non-rewarded trials within the reward condition, and (C) the improvement from baseline to non-rewarded trials scaled by the percentage of reward benefit accrued on non-rewarded trials.

stimulus–response-mappings have been associated with D_2 binding in caudate (Bäckman et al., 2011; Monchi et al., 2006). At the ROI level we found no significant differences in BP_{ND} from reward in caudate. However, voxelwise analyses revealed two clusters at a similar site bilaterally in anterodorsal caudate with lower BP_{ND} in the R condition. The left cluster overlapped with peak activation foci in a previous [^{11}C]raclopride PET study comparing switching to non-switching (Monchi et al., 2006). It is not clear whether the reward related change in BP_{ND} within caudate reflects a direct reward effect, or instead the reward-related enhancement in task updating that resulted in task performance enhancements. The difference between ROI and voxelwise analyses is likely due to the fact that our caudate and putamen ROIs ignored the functional subdivisions within the ROIs (Martinez et al., 2003). Alternatively, not enough time had passed for the reduction in caudate BP_{ND} to reach significance, as revealed by the trend when using the longer interval (frames 22-29).

The current findings may have been partially the result of a number of methodological decisions that were made in the current study. A critical factor was the use of a spatial high-resolution reconstruction algorithm that allowed inferences concerning small structures like NAcc. Spatial precision on the level of 3.1 mm^3 as offered by the Sharp IR OSEM reconstruction algorithm (Ross and Stearns, 2010) substantially reduces the risk that results are driven by partial volume effects from nearby regions. However, there have been reports that at high levels of statistical noise, or low radioactive concentrations, OSEM may introduce a bias, leading to an overestimation of ΔBP_{ND} (Walker et al., 2011). However, the present paradigm should be resistant to such a bias. First, we investigated only the striatum, a region with a high-affinity for [^{11}C]raclopride. Bias due to low regional uptake is more problematic when exploring extrastriatal ΔBP_{ND}. Second, whereas the amount of tracer rapidly decreases in bolus approaches, the B/I approach should be less affected since a fairly high level of tracer is maintained throughout the scan, although noise inevitably increases. To address this concern, the final four frames, likely more susceptible to potential bias, were removed from analysis. There are only a few investigations implementing high-resolution iterative reconstructions in combination with [^{11}C]raclopride (Alakurtti et al., 2013). Furthermore, there are no published studies evaluating the differential outcomes from adopting a bolus versus a B/I approach. High-resolution PET imaging enables smaller structures to be probed with greater precision, but its success depends on the validity of the reconstruction method. For instance, Alakurtti et al. (2013) succeeded in imaging the rostrocaudal gradients of D_2 receptor density in striatum. An important methodological goal is to further validate the effects of different methodological choices on reconstruction precision.

A second methodological decision was to use short rather than long frames throughout the session. This approach may be preferable,

despite the apparent disadvantage in causing higher frame-by-frame noise fluctuations. The gain in temporal resolution permits continued correction of the small remaining motion when using thermoplastic masks. The ability to correct for motion in PET imaging is vital in order to avoid false positive results (Egerton et al., 2009). This is especially important with the ~3 mm^3 PET resolution and the small NAcc volume, as well as in a lengthy paradigm where motion may change systematically depending on task demands. Motion correction should also benefit from maintaining higher levels of tracer with B/I.

The current results contribute to our understanding of the role of NAcc DA release in reward and cognition. In this regard, an important finding was the association of NAcc ΔBP_{ND} and improved task reaction time in the reward block. Hitherto, only one previous PET study has found a relation between rewarded task performance and ΔBP_{ND} in the striatal D_2 system (Koepp et al., 1998), but correcting for motion removed that relationship (Egerton et al., 2009). Nonetheless, memory performance has been associated with striatal D_2 receptor availability (i.e., rather than dynamic binding) in non-rewarded contexts (Bäckman et al., 2000; Cervenka et al., 2008). The individual-difference approach enabled us to investigate several associations between ΔBP_{ND} and task reaction time. Taken together these measures indicate whether participants change their effort depending on the presence of reward. Maintaining the same level of RT across trials indicates that effort is sustained across the reward block, whereas shifting between faster and slower responses depending on the presence of reward indicates that effort is transient and rather specific to rewarded trials. The first measure (R^+/R^- difference, Fig. 5B), implicitly assumes that NAcc would primarily reflect effort and RT during the R condition. The second measure (Fig. 5C) on the other hand assumes that NAcc DA reflects RT also during baseline and becomes bigger with increasingly speeding of R^- responses compared to baseline, and relative to the maximum reduction in RT achieved on R^+ trials. Of interest, higher NAcc DA release was negatively rather than positively correlated with transient reward-triggered RT improvements on R^+ relative to R^- trials. This pattern is not consistent with the view that NAcc ΔBP_{ND} reflects phasic DA release occurring preferentially on R^+ trials. Instead, the results are more consistent with the hypothesis that NAcc binding reflects tonic, rather than phasic, changes in DA during the R blocks, producing a global modulation of performance (i.e., on R^- as well as R^+ trials, thus reducing the RT difference between the two trial types). In support of this notion, NAcc was positively correlated with a behavioral index that reflects the degree to which RT improvements on R^- trials (relative to baseline) reflect the maximum improvement achieved throughout the reward block. The pattern resembles past findings (Beierholm et al., 2013; Jimura et al., 2010), in which changes in the reward motivational context produced global enhancements in behavioral performance (i.e., speeding of RT even on R^-/low reward trials).

The current findings are consistent with a number of theoretical accounts regarding the effects of reward motivation on cognitive performance. In the DMC framework (Braver, 2012), reward motivation is hypothesized to trigger DA release in PFC as well as striatum, with the PFC effects leading to changes in cognitive control due to enhanced updating and maintenance of task goals. According to the DMC account, enhancements of goal updating and maintenance are associated with a shift towards a proactive control strategy, in which performance would be enhanced consistently on all trials. Thus, according to the DMC account, the reward-related change in NAcc ΔBP_{ND} may serve as a marker of tonic DA release also occurring in PFC, which mediates the observed performance effects. In another theoretical account, known as the PBWM model, updating of task goals in working memory is mediated directly by the dorsal striatum (i.e., caudate), with phasic DA serving to optimize the timing of updating (O'Reilly and Frank, 2006). The observed changes in BP_{ND} in anterodorsal caudate are thus broadly consistent with this alternative account. Finally, theories regarding DA motivational effects provide an interpretation that is complementary to that of the DMC and PBWM accounts (Niv et al., 2006; Salamone and Correa, 2002; Sarter et al., 2006). On this view, rewarding motivational contexts lead to tonic increases of DA release in NAcc, which serve to enhance response vigor and attentional effort, specifically modulating cortical processing to optimize target-extraction and response readiness. According to this account, the observed changes in NAcc ΔBP_{ND} are consistent with a reward-triggered increase in response vigor and attentional effort, which jointly result in faster RTs.

Some potential limitations of the study, and more generally of the [^{11}C]raclopride PET dynamic-binding methodology, should be noted. First, although the presented results seem robust and conform to theory, the sample size was small (n = 11). Second, our caudate and putamen ROIs were not divided functionally (e.g. Martinez et al., 2003). This could be problematic in light of a large meta-analysis concluding that the division of striatal subregions influences results (Postuma and Dagher, 2006). Nevertheless, voxelwise analyses did reveal effects also in the dorsal caudate bilaterally and right ventral putamen. Furthermore, the NAcc ROI is a specific functional structure and was the primary target. Third, only one participant's structural MR image served as a ROI template. In order to avoid inclusion of regions outside the striatum, ROIs were thresholded on an individual basis. Conversely, there is no guarantee of including the entire striatum for all participants in the ROI template to begin with. Still, rather than increasing Type I errors this procedure should increase Type II errors. In addition, a strength of the present data is the concordant outcomes for NAcc ROI and voxelwise analyses. Finally, there was no control group performing the task-switching task without the additional reward. Hence, the reduction in BP_{ND} may be influenced by tracer washout, increased noise, or movement. Nevertheless, we did control for movement, both by realignment and use of a thermoplastic mask, and by discarding the last 10 min of the time series we further limited effects from these sources.

More generally, the [^{11}C]raclopride PET dynamic-binding method has limited temporal resolution and has selective sensitivity to D_2 binding. Disentangling the specific pathway in which D_2 binding relates to the dynamics of brain activity and task performance would require multimodal imaging, preferably by simultaneous use of PET and functional MRI. Additionally, complementary information regarding DA in PFC might be obtained from other radioligands that show greater sensitivity to D_1 receptors (which are predominant in PFC), such as [^{11}C]SCH23390 (Macdonald et al., 2012), or D_2 receptors, such as [^{18}F]fallypride (Ceccarini et al., 2012) or [^{11}C]FLB457 (Aalto et al., 2005).

In conclusion, motivation, associated with the limbic system and NAcc, is an intrinsic drive affecting both the initiation and enhancement of human behavior. Adopting a more complex task and with higher spatial resolution than former PET inquiries, subtle differences in NAcc BP_{ND} were detected during rewarded task switching. Our results complement existing accounts of reward and motivation, zooming in on NAcc as a key structure within VS in rewarding contexts. The functional role of NAcc DA release is less clear, however, but the present data indicate that it may have profound effects on behavioral performance even in task contexts with high cognitive control demands. Thoroughly answering that question would provide a major advance in motivational theory.

References

Aalto, S., Brück, A., Laine, M., Någren, K., Rinne, J.O., 2005. Frontal and temporal dopamine release during working memory and attention tasks in healthy humans: A positron emission tomography study using the high-affinity dopamine D2 receptor ligand [11C]FLB 457. J. Neurosci. 25, 2471–2477. http://dx.doi.org/10.1523/jneurosci.2097-04.2005.

Alakurtti, K., Johansson, J.J., Tuokkola, T., Någren, K., Rinne, J.O., 2013. Rostrocaudal gradients of dopamine D2/3 receptor binding in striatal subregions measured with [11C] raclopride and high-resolution positron emission tomography. NeuroImage 82, 252–259. http://dx.doi.org/10.1016/j.neuroimage.2013.05.091.

Bäckman, L., Ginovart, N., Dixon, R.A., Wahlin, T.B., Wahlin, A., Halldin, C., Farde, L., 2000. Age-related cognitive deficits mediated by changes in the striatal dopamine system. Am. J. Psychiatry 157, 635–637. http://dx.doi.org/10.1176/appi.ajp.157.4.635.

Bäckman, L., Nyberg, L., Soveri, A., Johansson, J., Andersson, M., Dahlin, E., Neely, A.S., Virta, J., Laine, M., Rinne, J.O., 2011. Effects of working-memory training on striatal dopamine release. Science 333, 718. http://dx.doi.org/10.1126/science.1204978.

Ballard, I.C., Murty, V.P., Carter, R.M., MacInnes, J.J., Huettel, S.A., Adcock, R.A., 2011. Dorsolateral prefrontal cortex drives mesolimbic dopaminergic regions to initiate motivated behavior. J. Neurosci. 31, 10340–10346. http://dx.doi.org/10.1523/jneurosci.0895-11.2011.

Beierholm, U., Guitart-Masip, M., Economides, M., Chowdhury, R., Düzel, E., Dolan, R., Dayan, P., 2013. Dopamine modulates reward-related vigor. Neuropsychopharmacology 38, 1495–1503. http://dx.doi.org/10.1038/npp.2013.48.

Braver, T.S., 2012. The variable nature of cognitive control: A dual mechanisms framework. Trends Cogn. Sci. 16, 106–113. http://dx.doi.org/10.1016/j.tics.2011.12.010.

Braver, T.S., Gray, J.R., Burgess, G.C., 2007. Explaining the many varieties of working memory variation: Dual mechanisms of cognitive control. In: Conway, A., Jarrold, C., Kane, M., Miyake, A., Towse, J. (Eds.), Variation in Working Memory. Oxford University Press, pp. 76–106. http://dx.doi.org/10.1093/acprof:oso/9780195168648.003.0004.

Carson, R.E., Breier, A., de Bartolomeis, A., Saunders, R.C., Su, T.P., Schmall, B., Der, M.G., Pickar, D., Eckelman, W.C., 1997. Quantification of amphetamine-induced changes in [11C]raclopride binding with continuous infusion. J. Cereb. Blood Flow Metab. 17, 437–447. http://dx.doi.org/10.1097/00004647-199704000-00009.

Ceccarini, J., Vrieze, E., Koole, M., Muylle, T., Bormans, G., Claes, S., Van Laere, K., 2012. Optimized in vivo detection of dopamine release using 18F-fallypride PET. J. Nucl. Med. 53, 1565–1572. http://dx.doi.org/10.2967/jnumed.111.099416.

Cervenka, S., Bäckman, L., Cselényi, Z., Halldin, C., Farde, L., 2008. Associations between dopamine D2-receptor binding and cognitive performance indicate functional compartmentalization of the human striatum. NeuroImage 40, 1287–1295. http://dx.doi.org/10.1016/j.neuroimage.2007.12.063.

Dahlin, E., Neely, A.S., Larsson, A., Bäckman, L., Nyberg, L., 2008. Transfer of learning after updating training mediated by the striatum. Science 320, 1510–1512. http://dx.doi.org/10.1126/science.1155466.

Egerton, A., Mehta, M.A., Montgomery, A.J., Lappin, J.M., Howes, O.D., Reeves, S.J., Cunningham, V.J., Grasby, P.M., 2009. The dopaminergic basis of human behaviors: A review of molecular imaging studies. Neurosci. Biobehav. Rev. 33, 1109–1132. http://dx.doi.org/10.1016/j.neubiorev.2009.05.005.

Fischl, B., Salat, D.H., Busa, E., Albert, M., Dieterich, M., Haselgrove, C., van der Kouwe, A., Killiany, R., Kennedy, D., Klaveness, S., Montillo, A., Makris, N., Rosen, B., Dale, A.M., 2002. Whole brain segmentation: Automated labeling of neuroanatomical structures in the human brain. Neuron 33, 341–355. http://dx.doi.org/10.1016/s0896-6273(02)00569-x.

Fonov, V., Evans, A.C., McKinstry, R.C., Almli, C.R., Collins, D.L., 2009. Unbiased nonlinear average age-appropriate brain templates from birth to adulthood. NeuroImage 47, S102. http://dx.doi.org/10.1016/s1053-8119(09)70884-5.

Fonov, V., Evans, A.C., Botteron, K., Almli, C.R., McKinstry, R.C., Collins, D.L., Group B.D.C., 2011. Unbiased average age-appropriate atlases for pediatric studies. NeuroImage 54, 313–327. http://dx.doi.org/10.1016/j.neuroimage.2010.07.033.

Haber, S.N., Knutson, B., 2010. The reward circuit: Linking primate anatomy and human imaging. Neuropsychopharmacology 35, 4–26. http://dx.doi.org/10.1038/npp.2009.129.

Haber, S.N., Fudge, J.L., McFarland, N.R., 2000. Striatonigrostriatal pathways in primates form an ascending spiral from the shell to the dorsolateral striatum. J. Neurosci. 20, 2369–2382 (http://www.jneurosci.org/content/20/6/2369).

Hakyemez, H.S., Dagher, A., Smith, S.D., Zald, D.H., 2008. Striatal dopamine transmission in healthy humans during a passive monetary reward task. NeuroImage 39, 2058–2065. http://dx.doi.org/10.1016/j.neuroimage.2007.10.034.

Innis, R.B., Cunningham, V.J., Delforge, J., Fujita, M., Gjedde, A., Gunn, R.N., Holden, J., Houle, S., Huang, S.C., Ichise, M., Iida, H., Ito, H., Kimura, Y., Koeppe, R.A., Knudsen, G.M., Knuuti, J., Lammertsma, A.A., Laruelle, M., Logan, J., Maguire, R.P., Mintun, M.A., Morris, E.D., Parsey, R., Price, J.C., Slifstein, M., Sossi, V., Suhara, T., Votaw, J.R., Wong, D.F., Carson, R.E., 2007. Consensus nomenclature for in vivo imaging of reversibly binding radioligands. J. Cereb. Blood Flow Metab. 27, 1533–1539. http://dx.doi.org/10.1038/sj.jcbfm.9600493.

Ito, H., Hietala, J., Blomqvist, G., Halldin, C., Farde, L., 1998. Comparison of the transient equilibrium and continuous infusion method for quantitative PET analysis of [11C] raclopride binding. J. Cereb. Blood Flow Metab. 18, 941–950. http://dx.doi.org/10.1097/00004647-199809000-00003.

Jimura, K., Locke, H.S., Braver, T.S., 2010. Prefrontal cortex mediation of cognitive enhancement in rewarding motivational contexts. Proc. Natl. Acad. Sci. U. S. A. 107, 8871–8876. http://dx.doi.org/10.1073/pnas.1002007107.

Knutson, B., Fong, G.W., Bennett, S.M., Adams, C.M., Hommer, D., 2003. A region of mesial prefrontal cortex tracks monetarily rewarding outcomes: Characterization with rapid event-related fMRI. NeuroImage 18, 263–272. http://dx.doi.org/10.1016/s1053-8119(02)00057-5.

Knutson, B., Taylor, J., Kaufman, M., Peterson, R., Glover, G., 2005. Distributed neural representation of expected value. J. Neurosci. 25, 4806–4812. http://dx.doi.org/10.1523/jneurosci.0642-05.2005.

Koepp, M.J., Gunn, R.N., Lawrence, A.D., Cunningham, V.J., Dagher, A., Jones, T., Brooks, D.J., Bench, C.J., Grasby, P.M., 1998. Evidence for striatal dopamine release during a video game. Nature 393, 266–268. http://dx.doi.org/10.1038/30498.

Krebs, R.M., Boehler, C.N., Roberts, K.C., Song, A.W., Woldorff, M.G., 2012. The involvement of the dopaminergic midbrain and cortico-striatal-thalamic circuits in the integration of reward prospect and attentional task demands. Cereb. Cortex 22, 607–615. http://dx.doi.org/10.1093/cercor/bhr134.

Lappin, J.M., Reeves, S.J., Mehta, M.A., Egerton, A., Coulson, M., Grasby, P.M., 2009. Dopamine release in the human striatum: Motor and cognitive tasks revisited. J. Cereb. Blood Flow Metab. 29, 554–564. http://dx.doi.org/10.1038/jcbfm.2008.146.

Laruelle, M., 2000. Imaging synaptic neurotransmission with in vivo binding competition techniques: A critical review. J. Cereb. Blood Flow Metab. 20, 423–451. http://dx.doi.org/10.1097/00004647-200003000-00001.

MacDonald, S.W., Karlsson, S., Rieckmann, A., Nyberg, L., Bäckman, L., 2012. Aging-related increases in behavioral variability: Relations to losses of dopamine D1 receptors. J. Neurosci. 32, 8186–8191. http://dx.doi.org/10.1523/jneurosci.5474-11.2012.

Martinez, D., Slifstein, M., Broft, A., Mawlawi, O., Hwang, D.R., Huang, Y., Cooper, T., Kegeles, L., Zarahn, E., Abi-Dargham, A., Haber, S.N., Laruelle, M., 2003. Imaging human mesolimbic dopamine transmission with positron emission tomography. Part II: Amphetamine-induced dopamine release in the functional subdivisions of the striatum. J. Cereb. Blood Flow Metab. 23, 285–300. http://dx.doi.org/10.1097/00004647-200303000-00004.

Martin-Soelch, C., Szczepanik, J., Nugent, A., Barhaghi, K., Rallis, D., Herscovitch, P., Carson, R.E., Drevets, W.C., 2011. Lateralization and gender differences in the dopaminergic response to unpredictable reward in the human ventral striatum. Eur. J. Neurosci. 33, 1706–1715. http://dx.doi.org/10.1111/j.1460-9568.2011.07642.x.

Monchi, O., Ko, J.H., Strafella, A.P., 2006. Striatal dopamine release during performance of executive functions: A [(11)C] raclopride PET study. NeuroImage 33, 907–912. http://dx.doi.org/10.1016/j.neuroimage.2006.06.058.

Niv, Y., Joel, D., Dayan, P., 2006. A normative perspective on motivation. Trends Cogn. Sci. 10, 375–381. http://dx.doi.org/10.1016/j.tics.2006.06.010.

Niv, Y., Daw, N.D., Joel, D., Dayan, P., 2007. Tonic dopamine: Opportunity costs and the control of response vigor. Psychopharmacology 191, 507–520.

O'Reilly, R.C., Frank, M.J., 2006. Making working memory work: A computational model of learning in the prefrontal cortex and basal ganglia. Neural Comput. 18, 283–328. http://dx.doi.org/10.1162/089976606775093909.

Pappata, S., Dehaene, S., Poline, J.B., Gregoire, M.C., Jobert, A., Delforge, J., Frouin, V., Bottlaender, M., Dolle, F., Di Giamberardino, L, Syrota, A., 2002. In vivo detection of striatal dopamine release during reward: A PET study with [(11)C]raclopride and a single dynamic scan approach. NeuroImage 16, 1015–1027. http://dx.doi.org/10.1006/nimg.2002.1121.

Pessoa, L., 2009. How do emotion and motivation direct executive control? Trends Cogn. Sci. 13, 160–166. http://dx.doi.org/10.1016/j.tics.2009.01.006.

Postuma, R.B., Dagher, A., 2006. Basal ganglia functional connectivity based on a meta-analysis of 126 positron emission tomography and functional magnetic resonance imaging publications. Cereb. Cortex 16, 1508–1521. http://dx.doi.org/10.1093/cercor/bhj088.

Rogers, R.D., Monsell, S., 1995. Costs of a predictable switch between simple cognitive tasks. J. Exp. Psychol. Gen. 124, 207–231. http://dx.doi.org/10.1037/0096-3445.124.2.207.

Ross, S., Stearns, C., 2010. SharpIR: White paper [PDF] URL http://www3.gehealthcare.com/~/media/downloads/us/product/product-categories/pet-ct/discovery-pet-ct-610/gehealthcare whitepaper_petct_sharpir.pdf?parent=%7bdd2081d8-e79d-4a7a-9408-89ded3e4d6b7%7d/.

Salamone, J.D., Correa, M., 2002. Motivational views of reinforcement: Implications for understanding the behavioral functions of nucleus accumbens dopamine. Behav. Brain Res. 137, 3–25. http://dx.doi.org/10.1016/s0166-4328(02)00282-6.

Salimpoor, V.N., van den Bosch, I., Kovacevic, N., McIntosh, A.R., Dagher, A., Zatorre, R.J., 2013. Interactions between the nucleus accumbens and auditory cortices predict music reward value. Science 340, 216–219. http://dx.doi.org/10.1126/science.1231059.

Sarter, M., Gehring, W.J., Kozak, R., 2006. More attention must be paid: The neurobiology of attentional effort. Brain Res. Rev. 51, 145–160. http://dx.doi.org/10.1016/j.brainresrev.2005.11.002.

Schott, B.H., Minuzzi, L., Krebs, R.M., Elmenhorst, D., Lang, M., Winz, O.H., Seidenbecher, C.I., Coenen, H.H., Heinze, H.J., Zilles, K., Düzel, E., Bauer, A., 2008. Mesolimbic functional magnetic resonance imaging activations during reward anticipation correlate with reward-related ventral striatal dopamine release. J. Neurosci. 28, 14311–14319. http://dx.doi.org/10.1523/jneurosci.2058-08.2008.

Schultz, W., 1998. Predictive reward signal of dopamine neurons. J. Neurophysiol. 80, 1–27 (http://jn.physiology.org/content/80/1/1).

Shen, Y.J., Chun, M.M., 2011. Increases in rewards promote flexible behavior. Atten. Percept. Psychophys. 73, 938–952. http://dx.doi.org/10.3758/s13414-010-0065-7.

Small, D.M., Gitelman, D., Simmons, K., Bloise, S.M., Parrish, T., Mesulam, M.M., 2005. Monetary incentives enhance processing in brain regions mediating top–down control of attention. Cereb. Cortex 15, 1855–1865. http://dx.doi.org/10.1093/cercor/bhi063.

Urban, N.B., Slifstein, M., Meda, S., Xu, X., Ayoub, R., Medina, O., Pearlson, G.D., Krystal, J.H., Abi-Dargham, A., 2012. Imaging human reward processing with positron emission tomography and functional magnetic resonance imaging. Psychopharmacology (Berl) 221, 67–77. http://dx.doi.org/10.1007/s00213-011-2543-6.

Walker, M.D., Asselin, M.C., Julyan, P.J., Feldmann, M., Talbot, P.S., Jones, T., Matthews, J.C., 2011. Bias in iterative reconstruction of low-statistics PET data: Benefits of a resolution model. Phys. Med. Biol. 56, 931–949. http://dx.doi.org/10.1088/0031-9155/56/4/004.

Watabe, H., Endres, C.J., Breier, A., Schmall, B., Eckelman, W.C., Carson, R.E., 2000. Measurement of dopamine release with continuous infusion of [11C]raclopride: Optimization and signal-to-noise considerations. J. Nucl. Med. 41, 522–530 (http://jnm.snmjournals.org/content/41/3/522.long).

Zald, D.H., Boileau, I., El-Dearedy, W., Gunn, R., McGlone, F., Dichter, G.S., Dagher, A., 2004. Dopamine transmission in the human striatum during monetary reward tasks. J. Neurosci. 24, 4105–4112. http://dx.doi.org/10.1523/jneurosci.4643-03.2004.